



## Subpicosecond Bunch Train Production for a Tunable mJ Level THz Source

S. Antipov,<sup>1,3</sup> M. Babzien,<sup>2</sup> C. Jing,<sup>1,3</sup> M. Fedurin,<sup>2</sup> W. Gai,<sup>3</sup> A. Kanareykin,<sup>1,5</sup> K. Kusche,<sup>2</sup>  
V. Yakimenko,<sup>2,\*</sup> and A. Zholents<sup>4</sup>

<sup>1</sup>*Euclid Techlabs LLC, Solon, Ohio 44139, USA*

<sup>2</sup>*Accelerator Test Facility, Brookhaven National Laboratory, Upton, New York 11973, USA*

<sup>3</sup>*High Energy Physics Division, Argonne National Laboratory, Lemont, Illinois 60439, USA*

<sup>4</sup>*Advanced Photon Source, Argonne National Laboratory, Lemont, Illinois 60439, USA*

<sup>5</sup>*St. Petersburg Electrotechnical University LETI, St. Petersburg 197376, Russia*

(Received 10 May 2013; published 25 September 2013)

A strong energy modulation in an electron bunch passing through a dielectric-lined waveguide was recently demonstrated in Antipov *et al.*, Phys. Rev. Lett. **108**, 144801 (2012). In this Letter, we demonstrate a successful conversion of this energy modulation into a beam density modulation, and the formation of a series of microbunches with a subpicosecond periodicity by means of magnetic optics (chicane). A strong coherent transition radiation signal produced by the microbunches is obtained and the tunability of its carrier frequency in the 0.68–0.9 THz range by regulating the energy chirp in the incoming electron bunch is demonstrated using infrared interferometry. A tabletop, compact, tunable, and narrow-band source of intense THz radiation based on this technology is proposed.

DOI: [10.1103/PhysRevLett.111.134802](https://doi.org/10.1103/PhysRevLett.111.134802)

PACS numbers: 41.60.Bq, 41.75.Ht, 41.85.Ct

In recent years there has been great interest in the production of series of equally spaced electron microbunches [1–5]. These series, referred to as microbunch trains, were considered for resonant excitation of the wakefields in plasma and dielectric wakefield accelerators [1,2], and for production of high power narrow band radiation with sub-THz carrier frequencies ([3–5], and references therein).

Several approaches have been considered for production of microbunch trains: (i) direct generation from a photocathode electron gun using a series of uniformly spaced laser pulses [5–7]; (ii) transverse to longitudinal phase space exchange in combination with a multislit mask [8–11]; (iii) difference frequency generation using double energy modulation of electrons in an undulator via interaction with optical lasers having slightly different carrier frequencies [12,13]; (iv) energy modulation by means of the self-excited wake fields in a dielectric-lined [14] or corrugated waveguide [15], and subsequent conversion into a density modulation. (We explore this technology further in this Letter.)

A strong energy modulation in an electron bunch passing through a dielectric-lined waveguide was recently demonstrated in [14]. Here, we report the successful conversion of the energy modulation into a density modulation and production of a picosecond bunch train. This result provides a foundation for the compact, tunable source of intense THz radiation proposed in Ref. [3].

When an ultrarelativistic electron propagates through a dielectric-lined tube it excites various waveguide modes with a phase velocity equal to electron velocity (the speed of light in the ultrarelativistic case). The frequency of the primary mode of interest, TM<sub>01</sub> mode synchronous with the beam can be calculated as [16]

$$f_1 \approx \frac{c}{2\pi} \sqrt{\frac{\epsilon}{\epsilon - 1}} \sqrt{\frac{2}{a\delta}}. \quad (1)$$

In the experiment we use capillaries (inner radius  $a = 300$  microns and wall thickness  $\delta = 28$  microns) made of kapton with dielectric permittivity ( $\epsilon = 3.3$ – $3.7$ ) [17,18]. For the numerical calculations in this Letter we assumed  $\epsilon = 3.5$  and  $f_1 = 0.805$  THz. In our experiment this mode dominates the wakefield excited by the sharp rise of the peak current at the leading edge of a 1.5 mm long quasirectangular electron bunch. Therefore, the wakefield inside such an electron beam is approximately a sine wave. Depending on the location along the electron bunch, electrons either gain or lose energy propagating through the waveguide and a longitudinal energy modulation along the beam is generated [14]. This energy modulation can be further transformed by appropriate beam optics into a density modulated beam, a bunch train.

A schematic of the experiment is presented in Fig. 1. The key components are the energy modulator described above, (section I) and a set of four dipole magnets, the chicane (section II). It is customary to characterize the chicane by its time-of-flight parameter  $R_{56}$  (the transfer matrix element describing chicane's longitudinal dispersion) that defines the path length difference as a function of the energy offset, i.e.,  $\Delta\ell = R_{56}(\Delta E/E)$  [19].

We consider beams with an energy chirp: energy linearly correlated with the longitudinal coordinate. Chirp is often measured in keV/mm, the correlated energy spread of the beam divided by its length. If the head of the bunch has a lower (higher) energy than the tail, the bunch is said to have a positive (negative) energy chirp. As shown in the chicane section II of Fig. 1 the higher energy trailing

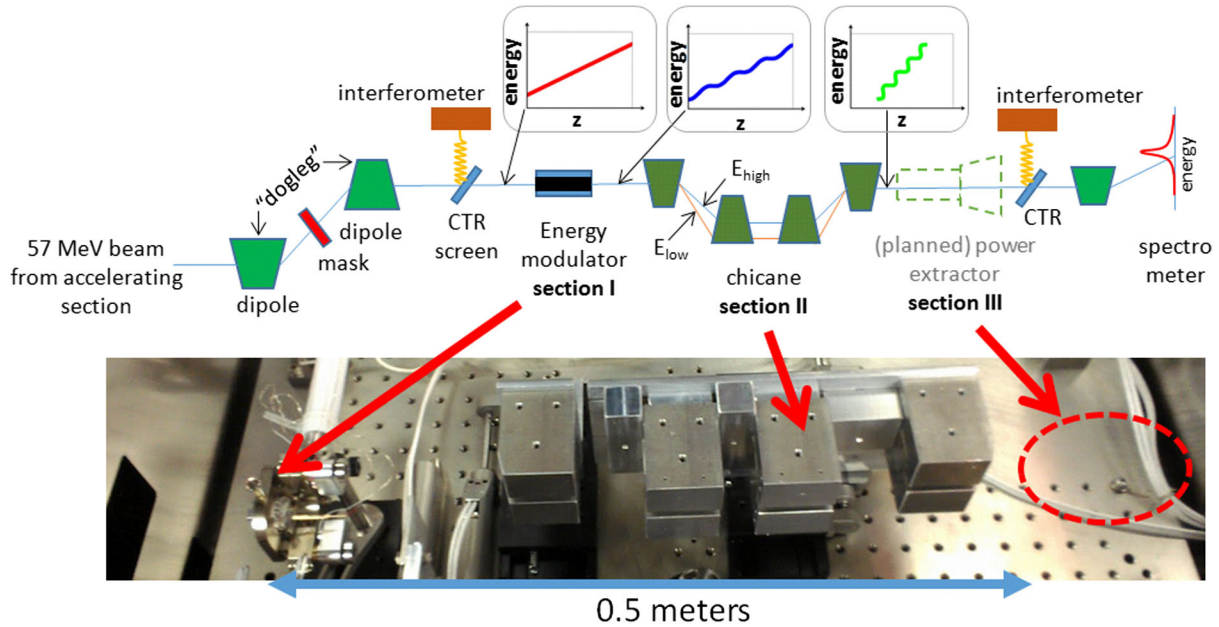


FIG. 1 (color online). The experimental setup. Section I is a movable stage containing a holder with a set of dielectric tubes that can be inserted into the beam as well as phosphor screens that are used for beam alignment. Section II contains the four permanent magnets forming the magnetic chicane, assembled on two movable stages as described in the text. Section III denotes a possible location for a radiator of the THz light and additional focusing lenses. Beam phase space manipulation is shown on the top.

electrons (in blue) travel a shorter distance in the chicane than the lower energy leading electrons (in red). If the energy chirp is positive (negative), then the electron bunch is compressed (stretched) after chicane. In the case of the beam with periodic energy modulation travelling through the chicane, a density modulation of the current appears. Figure 2 illustrates the process of formation of the density modulation. On the left we show the longitudinal phase space, where the red line represents the incoming electron bunch with the energy chirp. (For clarity, we ignore the incoherent energy spread that in this experiment was significantly smaller than the magnitude of the energy chirp.) The blue curve shows the same bunch undergoing energy

modulation after it exits the dielectric loaded waveguide. For an energy-modulated bunch there is a particular, “optimal” value of the matrix element  $R_{56}$  that produces the highest density modulation (the green curve in Fig. 2) with the bunching factor, a measure of density modulation of an electron beam,  $b = (1/N) \sum_{i=1}^N e^{ikz}$ , near 0.5.

The chicane not only forms a microbunch train out of the continuous bunch, but also compresses it as a whole. In Fig. 2 the extent of the projection of the green curve on the  $z$  axis is smaller than the extent of the blue curve’s projection. This effect leads to a frequency of the bunch train that is actually higher (1.5 THz in the example from Fig. 2), than the frequency of the energy-modulating self-wakefield

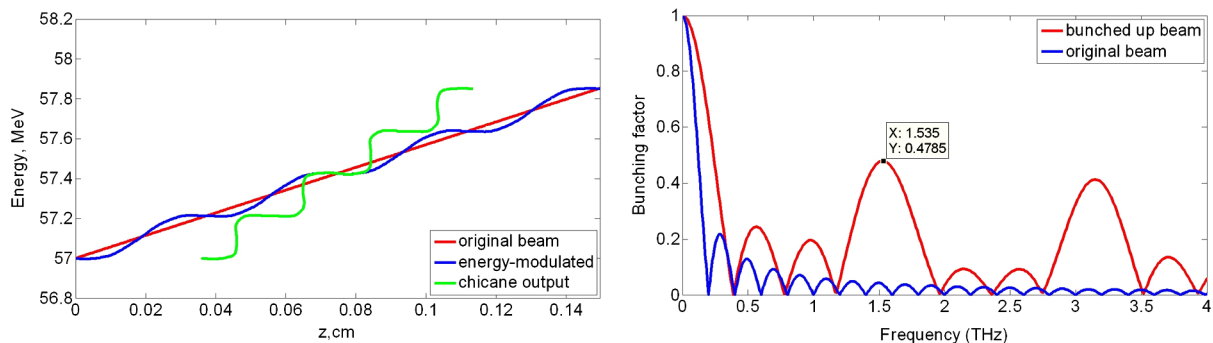


FIG. 2 (color online). Illustration for the process of bunching and compression. Left pane shows the longitudinal phase space portraits for the incoming electron bunch (red), energy modulated bunch (blue), and density modulated bunch after the chicane (green). The right pane shows the Fourier transform of the bunch density distribution before and after the chicane with the optimal value of the matrix element  $R_{56} = 4.9$  cm. Because of the positive energy chirp of the incoming electron bunch, the characteristic frequency of the bunch train (1.5 THz) is much higher than the characteristic frequency of the energy modulation (0.805 THz).

(0.805 THz, see below). A bunch without a chirp produces a bunch train with spacing equal to the wavelength of the energy-modulating structure.

The optimal value of the matrix element  $R_{56} = 4.9$  cm is rather large for experimental realization. The requirement on the strength of the chicane can be relaxed if the energy modulation is strong enough. We illustrate this with an example of an electron bunch with a negative chirp, Fig. 3. The energy modulation in this example is much stronger than in the previous case shown in Fig. 2. Because of the initial negative chirp the bunch is stretched after the chicane. We observe microbunching at a frequency of about 0.7 THz, lower than the energy-modulating structure mode frequency of 0.805 THz. Increasing  $R_{56}$  to the optimal level introduced above, lowers the bunch train frequency, Fig. 3. It is remarkable that by changing the energy chirp of the bunch, head-to-tail energy variation from 850 to  $-850$  keV, the output bunch train frequency can be varied from 0.7 to 1.5 THz using the same energy modulating structure, requiring only an adjustment of the chicane time-of-flight parameter [20] to obtain maximum bunching.

The experiment based on this concept was performed at the Accelerator Test Facility (ATF) at Brookhaven National Laboratory (BNL) [21]. The electron bunches provided by the ATF beam line at 57 MeV had a rectangular peak current profile with a length of  $\sim 5$  ps (1.5 mm) and amplitude of  $\sim 100$  A. The current distribution is produced by passing the beam through two dispersive dipole magnets with a mask in between that cuts off the tails [9]. The phase of the accelerating field in the linac was used to control a linear energy chirp along the electron bunch. The head-to-tail energy variation was as large as 850 keV in the experiment, similar to the theoretical examples given previously. For a 1.5-mm-long beam this would correspond to a chirp of 567 keV/mm. After acceleration, bunches were focused to a small transverse

size ( $\sim 100$   $\mu\text{m}$  rms) and transported through a 2-in.-long metallized on the outside kapton (polyimide) tube with a 300 micron inner radius and 28 micron wall thickness. The kapton has nearly constant permittivity  $\epsilon$  in the range of frequencies between 0.5 and 1.5 THz [17,18]. The chicane was made out of four identical permanent dipole magnets. Each magnet has 5 cm magnetic length and  $\sim 9.4$  kG maximum magnetic field for a 5 mm magnetic gap. The distance between the first and the second magnet and the third and the fourth was 5 cm. This chicane had the matrix element value  $R_{56} = 1$  cm. We were able to move chicane in and out of the beam line so that it was possible to measure the electron bunch properties both with and without the presence of the chicane.

After the bunch passes through sections I and II of the experimental setup it becomes density modulated and this modulation can be measured by passing the bunch through a foil producing coherent transition radiation (CTR) and analyzing the time structure of the signal with a Michelson interferometer using a bolometer as the detector [2,9,11]. The result of the interferometric measurement is the auto-correlation function (intensity as a function of the path length difference in the interferometer) of the CTR signal that has a periodicity related to the periodicity of electron bunch. However, the exact spectrum of the signal is rather hard to obtain because of dispersive elements in the THz transport and measurement line. The vacuum window through which the CTR signal exits the beam line, the interferometer, and the bolometer used for the actual intensity measurement, all have different responses depending on the frequency of the signal. The goal of the experiment was to demonstrate the general principles of proposed bunch train production. The resulting bunching can be clearly observed through periodicity of the auto-correlation function. Figure 4 compares interferometric measurements of the original bunch (chicane retracted) and the density modulated bunch for various values of

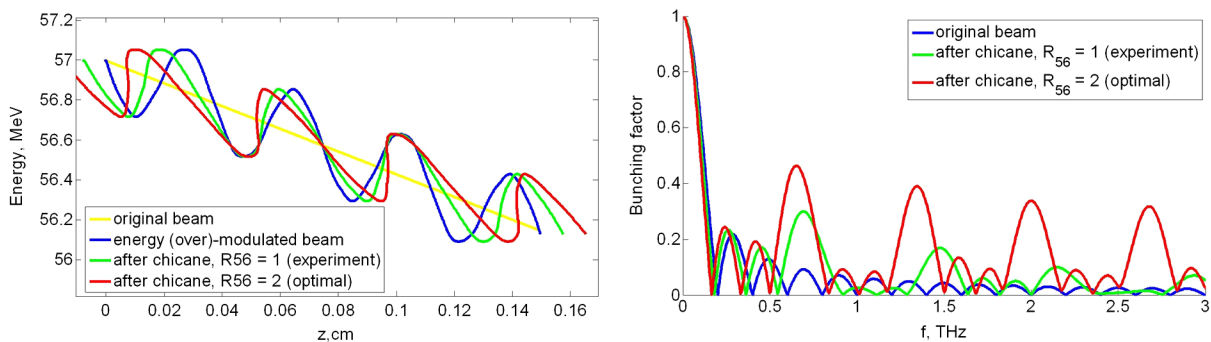


FIG. 3 (color online). Illustration for bunching and stretching. The left pane shows the longitudinal phase space of the original bunch (yellow), the energy modulated bunch (blue), and the density modulated bunch after the chicane (green and red). The right pane shows the bunch frequency content before and after the chicane. A negative slope on the energy chirp leads to a bunch train frequency (0.7 THz) lower than the frequency of the energy modulating structure (0.805 THz). We also compare results from an optimal chicane (red curves) to that used in the experiment (green curves). It is particularly important in this case that the energy modulation is not perfect, i.e., the bunch is over-modulated. This allows us to use a small value of the matrix element  $R_{56}$  to obtain a high bunching factor  $\sim 0.3$ .

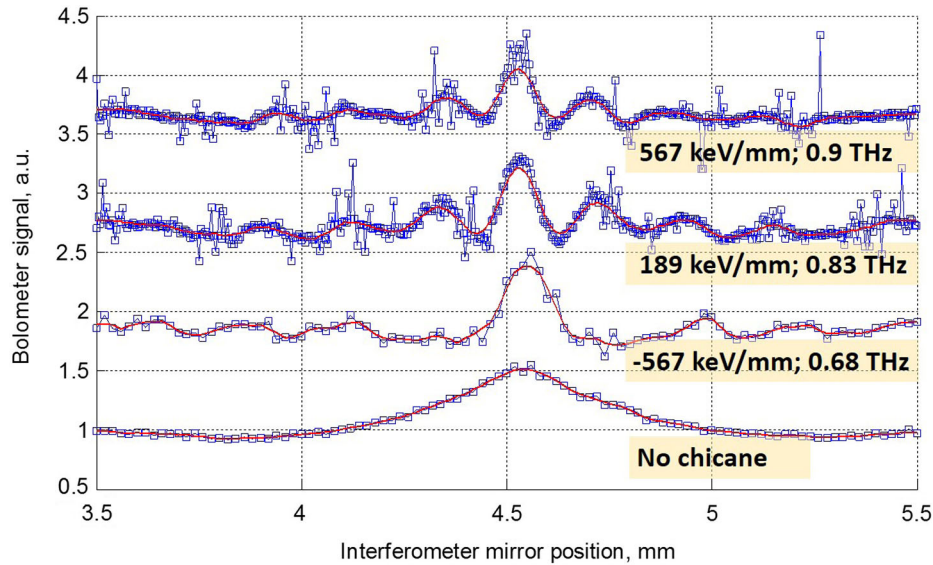


FIG. 4 (color online). Measured THz CTR signal for various energy chirp values. Autocorrelation function from the interferometric measurement: squares correspond to raw data, and the solid line represents the smoothed fit. Cases (from top to bottom): 567, 189, and  $-567$  keV/mm energy chirp and no-chicane case.

the energy chirp. The autocorrelation function is periodic for a signal produced by the density modulated beam, while the original long rectangular bunch does not produce periodicity over the distance spanned by interferometer mirror motion. We can also conclude that there are 4 beamlets in the density modulated beam (bunch train) because we have 7 pronounced peaks on the autocorrelation function plot. This determines the bandwidth of the signal to be about 25%. As described above, depending on the bunch energy chirp we can produce bunch trains with variable frequencies. In the experiment we varied the linac phase to obtain chirp values ranging from  $-567$  to  $567$  keV/mm. The autocorrelation function measurements show that we were able to change the bunch train periodicity from an estimated 0.68 to 0.9 THz, correspondingly (Fig 4).

We were not able to observe bunch train production at small energy chirps. In this case the small energy chirp becomes comparable to the bunch intrinsic energy spread and the induced energy modulation is overshadowed by the overall spread. We did not directly measure the energy per pulse of the THz signal produced by the coherent transition radiation.

Finally, based on this demonstrated technique for production of the bunch train we propose a compact, tunable, and a narrow bandwidth source of THz radiation. All components are similar to those used in this experiment but adjusted to the specific needs of a dedicated THz radiation source. An electron bunch is produced in the gun and accelerated to a few MeV offcrest forming an energy chirp along the electron bunch. After that it passes through a dogleg (two dipole magnets of equal strength and opposite sign, Fig. 1) where a collimator is used to cut the bunch tails and to provide a uniform density distribution

with a relatively sharp leading edge [9]. Next, similar to the experiment above, this bunch traverses the energy modulating structure, section I, Fig. 1. In section II (chicane) the energy modulation acquired is converted into a density modulation. The resulting bunch train is further injected into the power extractor, which is essentially another wakefield producing structure that is a dielectric loaded or corrugated metal waveguide equipped with a horn-type antenna. Additional electron focusing optics may be needed to control the beam size as it loses energy in the extractor.

Wide tunability of this THz source is realized through control of the energy chirp as it was demonstrated in this experiment. It is also possible to use a planar dielectric loaded or a corrugated metallic waveguide for the energy modulating structure; this permits adjustment of the frequency of the fundamental mode by varying the waveguide vacuum gap. The matrix element  $R_{56}$  of the second chicane needs to be adjustable to optimize the bunching efficiency [20]. The power extractor will be tuned to the bunch train frequency, which can be done in a similar fashion to the energy modulator. In principle, other radiators like a thin foil, grating, or undulator could be used. The latter has the advantage that it could amplify the seed signal using the FEL amplification mechanism.

We have designed two THz power extraction structures for possible experiments at the BNL ATF [21] and at the Argonne Wakefield Accelerator (AWA) facility [22], assuming realistic bunch train parameters for each facility. Using these parameters we calculate the THz pulse peak power and pulse length and obtain the total energy in a pulse [23]. For the 800 pC, 100 A, 57 MeV ATF beam we use a 3 cm long quartz tube with ID = 0.3 mm and

OD = 0.4 mm to produce a 0.7 THz, 170 ps long pulse with a peak power of 6 MW and 1 mJ energy/pulse. A high-charge bunch train at the AWA produces a 0.75 GV/m field inside a quartz tube with ID = 1 mm and OD = 1.2 mm. A 10 cm long structure can decelerate the 75 MeV bunch virtually to zero, radiating 0.3 J into a 0.3 THz signal with a 330 ps pulse length. Repetition rate, hence average THz power, is determined by the accelerator. While facilities like ATF and AWA have repetition rates on the order of 10 Hz, new FEL machines are geared towards 100 kHz and even 1 MHz. In the case of high repetition rate operation thermal management of the structure is necessary. In [24] an 850 GHz structure was considered for a FEL application at 100 kHz. In the THz region wake attenuation is rather high, especially considering small capillary structures, however, power dissipation was shown to be still manageable for the water cooling technology [24]. In practical devices one can trade off the output power with compactness and/or tuning capabilities.

Euclid Techlabs LLC acknowledges support from the DOE SBIR program Grant No. DE-SC0006299 and U.S. Department of Energy Office of Science under Contract No. DE-AC02-06CH11357. The authors thank G. Andonian, O. Williams, S. Barber, B. O'Shea, and J. Rosenzweig of UCLA for providing the RadiaBeam BLIS interferometer and other essential experimental hardware.

---

\*Present address: SLAC National Accelerator Laboratory, Menlo Park, California 94025, USA.

- [1] E. Kallos, T. Katsouleas, W.D. Kimura, K. Kusche, P. Muggli, I. Pavlishin, I. Pogorelsky, D. Stolyarov, and V. Yakimenko, *Phys. Rev. Lett.* **100**, 074802 (2008).
- [2] G. Andonian, O. Williams, X. Wei, P. Niknejadi, E. Hemsing, J.B. Rosenzweig, P. Muggli, M. Babzien, M. Fedurin, K. Kusche, R. Malone, and V. Yakimenko, *Appl. Phys. Lett.* **98**, 202901 (2011).
- [3] S. Antipov, C. Jing, P. Schoessow, A. Kanareykin, V. Yakimenko, A. Zholents, and W. Gai, *Rev. Sci. Instrum.* **84**, 022706 (2013).
- [4] G.L. Carr, M. Martin, W. McKinney, K. Jordan, G. Neil, and G. Williams, *Nature (London)* **420**, 153 (2002).
- [5] J. Neumann, R. Fiorito, P. O'Shea, H. Loos, B. Sheehy, Y. Shen, and Z. Wu, *J. Appl. Phys.* **105**, 053304 (2009).
- [6] M. Boscolo, M. Ferrario, I. Boscolo, F. Castelli, and S. Cialdi, *Nucl. Instrum. Methods Phys. Res., Sect. A* **577**, 409 (2007).
- [7] J. Power and C. Jing, *AIP Conf. Proc.* **1086**, 689 (2009).
- [8] Y.-E. Sun, P. Piot, A. Johnson, A.H. Lumpkin, T.J. Maxwell, J. Ruan, and R. Thurman-Keup, *Phys. Rev. Lett.* **105**, 234801 (2010).
- [9] P. Muggli, V. Yakimenko, M. Babzien, E. Kallos, and K.P. Kusche, *Phys. Rev. Lett.* **101**, 054801 (2008).
- [10] Y.C. Du, W.H. Huang, and C.X. Tang, *Chinese Phys. C* **36**, 151 (2012).
- [11] P. Piot, Y.-E. Sun, T.J. Maxwell, J. Ruan, A.H. Lumpkin, M.M. Rihaoui, and R. Thurman-Keup, *Appl. Phys. Lett.* **98**, 261501 (2011).
- [12] D. Xiang and G. Stupakov, *Phys. Rev. ST Accel. Beams* **12**, 080701 (2009).
- [13] M. Dunning, C. Hast, E. Hemsing, K. Jobe, D. McCormick, J. Nelson, T.O. Raubenheimer, K. Soong, Z. Szalata, D. Walz, S. Weathersby, and D. Xiang, *Phys. Rev. Lett.* **109**, 074801 (2012).
- [14] S. Antipov, C. Jing, M. Fedurin, W. Gai, A. Kanareykin, K. Kusche, P. Schoessow, V. Yakimenko, and A. Zholents, *Phys. Rev. Lett.* **108**, 144801 (2012).
- [15] K. Bane and G. Stupakov, *Nucl. Instrum. Methods Phys. Res., Sect. A* **677**, 67 (2012).
- [16] K. Bane and A. Novokhatskii, LCLS Report No. LCLS TN-99-1, 1999.
- [17] C. Stoik, Ph.D. thesis, Air Force Institute of Technology, 2008.
- [18] M. Ree, K. J. Chen, D. P. Kirby, N. Katzenellenbogen, and D. Grischkowsky, *J. Appl. Phys.* **72**, 2014 (1992).
- [19] H. Wiedemann, *Particle Accelerator Physics* (Springer, New York, 2008).
- [20] S. Antipov, C. Jing, P. Schoessow, A. Kanareykin, W. Gai, A. Zholents, M. Fedurin, K. Kusche, V. Yakimenko, and B. Jiang, *Proceedings of the International Particle Accelerator Conference (IPAC'12), New Orleans, LA, 2012* (IEEE, New York, 2012), pp. 595–597.
- [21] V. Yakimenko, *AIP Conf. Proc.* **737**, 677 (2004).
- [22] M. Conde, S. Antipov, W. Gai, C. Jing, R. Konecny, W. Liu, J.G. Power, H. Wang, and Z. Yusof, *AIP Conf. Proc.* **737**, 657 (2004).
- [23] F. Gao, M.E. Conde, W. Gai, C. Jing, R. Konecny, W. Liu, J.G. Power, T. Wong, and Z. Yusof, *Phys. Rev. ST Accel. Beams* **11**, 041301 (2008).
- [24] C. Jing, A. Kanareykin, J. Power, and A. Zholents, *Proceedings of the International Particle Accelerator Conference (IPAC'11), San Sebastian, Spain, 2011* (IEEE, New York, 2011), pp. 1485–1487.